1987

NASA/ASEE SUMMER FACULTY RESEARCH FELLOWSHIP PROGRAM

MARSHALL SPACE FLIGHT CENTER
THE UNIVERSITY OF ALABAMA IN HUNTSVILLE

AN INVESTIGATION OF OBLIQUE HYPERVELOCITY IMPACT

Prepared By:	William P. Schonberg
Academic Rank:	Assistant Professor
University and Department:	The University of Alabama in Huntsville Mechanical Engineering
NASA/MSFC:	
Laboratory:	Materials and Processes
Division:	Engineering Physics
Branch:	Laboratory Support
NASA Colleague:	Roy Taylor
Date:	August 17, 1987
Contract No:	The University of Alabama in Huntsville NGT-01-008-021

ABSTRACT

This report describes the results of an experimental investigation of phenomena associated with the oblique hypervelocity impact of spherical projectiles on multi-sheet aluminum structures. A model that can be employed in the design of meteoroid and space debris protection systems for space structures is developed. The model consists of equations that relate crater and perforation damage of a multi-sheet structure to parameters such as projectile size, impact velocity, and trajectory obliquity. The equations are obtained through a regression analysis of oblique hypervelocity impact test data. This data shows that the response of a multi-sheet structure to oblique impact is significantly different from its response to normal hypervelocity impact. It was found that obliquely incident projectiles produce ricochet debris that can severely damage panels or instrumentation located on the exterior of a space structure. Obliquity effects of high-speed impact must, therefore, be considered in the design of any structure exposed to the hazardous meteoroid and space debris environment.

INTRODUCTION

All spacecraft with a mission duration of more than a few days are susceptible to impacts by meteoroid and pieces of orbiting space debris. These impacts occur at high speeds and can damage flight-critical systems of a spacecraft. This damage can in turn lead to catastrophic failure of the spacecraft. Therefore, the design of a spacecraft for a long-duration mission must take into account the effects of such impacts on the spacecraft structure and all of its exposed subsystem components, such as solar arrays and instrumentation units.

Until recently, meteoroid impact was better understood and believed to be more serious than the impact of orbital space debris. However, recent studies and workshops on orbital debris have determined that orbital debris is becoming an increasingly serious hazard to long-duration near-earth space missions (see, e.g., Kessler and Su, 1985; Reynolds, et.al., 1983; and, Kessler, 1981). In certain regions of earth orbit the threat of orbital debris impact now exceeds the threat posed by meteoroid impact. It is evident from these and other studies that the orbital debris problem is serious, and that the probability of collision is rising as the orbital population increases. Protective systems must be developed in order to insure the safety of a spacecraft hull and its occupants, as well as the integrity of its exterior subsystems when encountering the meteoroid and space debris environment.

The design of meteoroid/space debris protection systems depends largely on the ability to predict the behavior of a variety of structural components under conditions of meteoroid or space debris impact. Forty years ago it was suggested that 'meteoroid bumpers' could be used to minimize the damage caused by the high-speed impact of meteoroids (Whipple, 1947). Since then, numerous experimental and analytical investigations have been performed to determine the resistance of multi-sheet structures to hypervelocity impact (see, e.g., Swift, 1983; Wilkinson, 1969; Lundeberg, et.al., 1966; Maiden and McMillan, 1964; and, Wallace, et.al., 1962). In the majority of the experimental studies, the trajectories of the high-speed projectiles were normal to the surface of the structures. However, it has become increasingly evident that most meteoroid or space debris impacts will not occur normal to the surface of a spacecraft. Unfortunately, information on oblique hypervelocity impact is relatively scarce so that it is difficult to assess the severity of such impacts on a structure or subsystem component. Studies of oblique impact that have been performed typically do not discuss the possibility of ricochet damage to external systems (see, e.g., Johnson, 1969; McMillan, 1968; Burch, 1967; and, Summers, 1959).

OBJECTIVES

To increase the understanding of phenomena associated with oblique hypervelocity impact, a program of research was developed at the Marshall Space Flight Center. The objective of this program was to generate and analyze oblique hypervelocity impact test data. The results of this research program are presented in this report.

In the first section, a review of the experimental procedure used in the oblique hypervelocity impact testing of multi-sheet structures is presented. In the next section, impact test results are reviewed qualitatively. In the following sections, the test data obtained are reduced and analyzed. The analysis indicates that perforation and ricochet trajectories, as well as bumper hole dimensions, can be correlated as functions of the impact parameters of the original projectile and the geometrical properties of the projectile/multi-sheet specimen system. A preliminary investigation of ricochet damage is performed to determine probable sizes and velocities of ricochet particles. In the final section, conclusions are made based on the analysis of the data and visual inspection of the damaged specimens. Recommendations for future experimental and analytical investigations of oblique hypervelocity impact are also presented.

EXPERIMENTAL PROCEDURE AND RESULTS

The oblique hypervelocity impact testing of multi-sheet specimens was done at the Space Debris Simulation Facility of the Materials and Processes Laboratory at the Marshall Space Flight Center. The Facility consists of a light gas gun with a 12.7 mm launch tube capable of launching 2.5 - 12.7 mm projectiles of mass 4 - 300 mg at velocities of 2 - 8 km/sec. Projectile velocity measurements were accomplished via pulsed X-ray, laser diode detectors, and a Hall photographic station. The light gas gun has three target tanks with interior volumes of 0.067, 0.53, and 28.5 cubic meters. The multi-sheet specimen set-up is shown in Figure 1. The specimens and the conditions of impact were chosen to simulate the conditions of space debris impact as closely as possible and still remain within the realm of experimental feasibility.

In each test, an spherical projectile of diameter D impacted a bumper plate of thickness t_S with a velocity V and at an angle of obliquity θ. The projectile was shattered upon impact and created an elliptical hole in the bumper plate. Some secondary projectile and bumper plate fragments were sprayed upon the pressure wall plate a distance S away while some fragments ricocheted and struck the ricochet witness plate (thickness t_R). The angles θ_1 and θ_2 are 'perforation angles' and denote the trajectories of bumper and 'in-line' projectile fragments, respectively. The angles α_c and α_{99} are 'ricochet angles' and denote the trajectory of the center of mass of the ricochet fragments and the angle below which lie 99% of the ricochet fragments, respectively.

The projectiles used were solid 1100 aluminum spheres of diameter 4.75 mm, 6.35 mm, and 7.95 mm. The bumper, pressure wall, and ricochet witness plates were made of 6061-T6, 2219-T87, and 2219-T6 aluminum, respectively. Their thicknesses were held constant at 1.5875 mm, 3.175 mm, and 2.54 mm, respectively. The angles of obliquity ranged from 30 to 75 degrees, and the test impact velocities ranged from 5.0 to 7.5 km/sec. The bumper and pressure wall plates were separated by a constant distance of 10.16 mm. A total of 22 test specimens were used to study the penetration and ricochet phenomena.

The results of the test firings are presented in Table 1. The angles θ_1 and θ_2 were obtained by estimating the locations of the centers of mass of the bumper fragments and 'in-line' projectile fragments on the pressure wall plate. The angle α_c was obtained by determining the vertical location of the center of mass of the ricochet debris based on the vertical distribution of the holes, craters, etc. formed by the debris. The angle α_{99} was determined based on the height below which lay 99% of the holes, craters, etc. formed by the ricochet debris. The minimum and maximum dimensions of the bumper plate hole, D_{min} and D_{max}, respectively, were measured directly from the bumper plate. Examples of damaged test specimens for various angles of obliquity are presented in Figures 2 through 5. Visual inspection of these and other test plates

revealed several interesting features in each of three obliquity regimes.

Low Obliquity Regime (0-deg < θ <45-deg)

For the impact tests in which the angle of obliquity was 30 degrees, there was extensive damage to the pressure wall plate but virtually no damage to the ricochet witness plate (Figues 2b and 2c). The pressure wall plate damage strongly resembled the damage observed during normal impact. Furthermore, the trajectory of the center of mass of the projectile fragments was very close to the original impact trajectory. The hole in the bumper plate was elliptical, with an eccentricity close to 1.0 (Figure 2a).

Medium Obliquity Regime (45-deg < θ < 60-deg)

The damaged pressure wall plates shown in Figures 3b and 3c are typical of test specimens in which the trajectory obliquity of the original projectile was greater than 45 degrees. Two distinct areas of damage are discernable on the plates. The damage areas on the left contain craters and holes that are nearly circular, which is characteristic of normal impact. The craters in the damage areas on the right are oblong, indicating that they were formed by oblique impacts. From these considerations, it became possible to differentiate between pressure wall plate damage caused by bumper plate fragments (circular craters and holes) and damage caused by projectile fragments (oblong craters and holes). As the trajectory obliquity of the original projectile was increased, the trajectories of the bumper plate and projectile fragments were observed to separate even more. The trajectory of the bumper fragments began to approach the normal line between the bumper and pressure wall plate while the trajectory of the projectile fragments, although no longer 'in-line' with the original trajectory, was still relatively close to it. The bumper plate hole was still elliptical with a steadily increasing eccentricity (see Figures 3a and 4a).

High Obliquity Regime (60-deg < θ < 75-deg)

With further increases in obliquity, an increasing amount of cratering and perforation was observed on the ricochet witness plates. Up to a certain critical angle, the most serious damage was still observed on the pressure wall plate, with the ricochet witness plate sustaining a relatively low level of damage (Figures 3b,c and 4b,c). However, once the critical angle was exceeded, the ricochet witness plate began to exhibit excessive cratering and perforation while the damage to the pressure wall plate decreased dramatically (Figure 5c). This critical angle is estimated to have a value between 60 and 65 degrees. At obliquities beyond this critical angle, the trajectory of the shield fragments was virtually normal to the pressure wall plate and the trajectory of the projectile fragments was severely departed from the original trajectory of the impacting projectile (Figure 5b). The bumper plate hole, although still elongated, ceased to be elliptical and developed a flattened end at the end nearest to the ricochet witness plate (Figure 5a). This indicates the that a projectile incident at a high angle of obliquity will tear, as well as shatter, the bumper plate upon impact.

BUMPER PLATE HOLE ANALYSIS

Elastodynamic theory predicts that as a hypervelocity projectile impacts a protective bumper plate, the projectile and the portion of the plate surrounding the impact site will break up into many fragments (Cour-Palais, 1979). In order to be able to predict the damage capability of these fragments, it is necessary to know the volume of debris that will be produced as a result of the impact. A good estimate of the volume of bumper plate fragments can be obtained by calculating the area of the hole created during the impact. Inspection of the test specimens revealed the bumper plate hole to be elliptical with the elongation along the horizontal projection of the original projectile trajectory (Figures 2a, 3a, 4a, and, 5a). The bumper plate hole area can be, therefore, approximated as the area of an ellipse having major and minor axes equal to the maximum and minimum transverse hole dimensions, respectively. The objective of this analysis was to obtain empirical equations that relate these hole dimensions to impact parameters such as velocity, angle of obliquity, and projectile diameter.

Inspection of the hole size data in Table 1 reveals several interesting features. First, the size of the minimum dimension, D_{min}, appears to be relatively independent of the angle of obliquity. The maximum dimension, D_{max}, however, appears to be strongly dependent on trajectory obliquity.

Based on these observations, the first task in the analysis was to determine whether exisiting equations that predict bumper hole diameters in normal high-speed impacts could be used to predict either dimension of the holes formed in oblique impact. A survey of the literature revealed six equations for hole diameter under normal impact. They are listed in the Appendix. The equations developed by Maiden, et.al. (1963) for normal impact were found to predict the minimum hole dimension under oblique impact rather well (See Table 2). However, no single equation was able to accurately predict the maximum hole dimension, even for small trajectory obliquities. This is not surprising considering the strong dependence of D_{max} on the initial trajectory obliquity of the projectile.

The second task undertaken was to independently derive empirical equations for the maximum and minimum hole dimensions as functions of the projectile diameter, impact velocity, and angle of obliquity. Because the minimum hole dimension is relatively independent of trajectory obliquity, an obliquity correction term was included only in the equation for the maximum hole dimension. The equations were obtained through standard multiple linear regression techniques with the following results:

$$D_{min}/D = 2.794\ (V/C)^{0.962}\ (t_s/D)^{0.895} + 1.120 \qquad (1)$$

$$D_{max}/D = 4.575\ (V/C)^{0.450}\ (\sin\theta)^{1.303}\ (t_s/D)^{0.672} + 1.470 \qquad (2)$$

where C is the speed of sound in the bumper plate material. The average prediction errors and correlation coefficients of the regression model are presented in Table 3 (columns 1 and 2, respectively). The equations are a fairly good fit to the hole dimension data and have a small average prediction error. It should be noted that these equations are valid only for projectiles and plates made of the same material.

PERFORATION ANGLE ANALYSIS

The perforation angles θ_1 and θ_2 were obtained by estimating the locations of the centers of mass of the bumper fragment sprays and the 'in-line' projectile fragment sprays on the pressure wall plates of the impacted specimens. Empirical expressions for θ_1 and θ_2 were obtained first as functions of the bumper plate hole dimensions, and then as functions of projectile diameter, impact velocity and trajectory obliquity. The equations were obtained through standard multiple linear regression techniques with the following results:

As functions of bumper hole dimensions:

$$\theta_1/\theta = 0.697\ (V/C)^{0.277}\ (D_{min}/D)^{0.246}\ (D_{max}/D)^{-1.463} \quad (3)$$

$$\theta_2/\theta = 1.518\ (V/C)^{0.034}\ (D_{min}/D)^{-0.733}(D_{max}/D)^{-0.105} \quad (4)$$

As functions of original impact parameters:

$$\theta_1/\theta = 0.085\ (V/C)^{0.149}\ (\sin\theta)^{-1.744}\ (t_S/D)^{-0.233} \quad (5)$$

$$\theta_2/\theta = 0.427\ (V/C)^{-0.318}(\sin\theta)^{-0.225}\ (t_S/D)^{-0.436} \quad (6)$$

The average prediction errors and correlation coefficients are presented in Table 4. Inspection of the correlation coefficients reveals that the θ_2 data did not regress as well as the θ_1 data. This is in part due to the fact that the 'in-line' trajectory angle, θ_2, is not a single-valued function of trajectory obliquity, θ. It can be seen in Figure 6 that θ_2 varies directly with θ up to a critical value, θ_{cr}, between 60 and 65 degrees and then decreases with further increases in θ. This reversal at $\theta = \theta_{cr}$ corresponds to a change in the location of the most severe damage from the pressure wall plate for $\theta < \theta_{cr}$ to the ricochet witness plate for $\theta > \theta_{cr}$. This multi-valued behavior of θ_2 and its effect on the behavior of θ_1 will be examined at a future time. As such, equations (3) through (6) are applicable only for angles of obliquity between 0 and 65 degrees. It should again be noted that these equations are valid only for projectiles and plates of the same material. Furthermore, the data used in the regression analysis itself may have an error of ±1 or ±2 percent due to the difficulty in determining the exact locations on the pressure wall plate of the centers of mass of the particle sprays.

RICOCHET ANGLE ANALYSIS

The ricochet angle α_c was obtained by determining the vertical location of the center of mass of the ricochet debris based on the vertical distribution of the holes, craters, etc., formed by the debris on the ricochet witness plate. The angle α_{99} was determined based on the height below which lay 99% of the holes, craters, etc. formed by the ricochet debris. Empirical expressions for α_c and α_{99} were obtained as first as functions of the bumper plate hole dimensions, and then as functions of projectile diameter, impact velocity and trajectory obliquity. The equations were obtained through standard multiple linear regression techniques with the following results:

As functions of bumper hole dimensions:

$$\alpha_c/\theta = 2.196\ (V/C)^{1.079}\ (D_{min}/D)^{-0.288}\ (D_{max}/D)^{-2.295} \quad (7)$$

$$\alpha_{99}/\theta = 2.381\ (V/C)^{0.465}\ (D_{min}/D)^{0.185}\ (D_{max}/D)^{-1.762} \quad (8)$$

As functions of original impact parameters:

$$\alpha_c/\theta = 0.030\ (V/C)^{0.898}\ (\sin\theta)^{-2.892}\ (t_S/D)^{-0.685} \quad (9)$$

$$\alpha_{99}/\theta = 0.169\ (V/C)^{0.431}\ (\sin\theta)^{-2.072}\ (t_S/D)^{-0.291} \quad (10)$$

The average prediction errors and correlation coefficients are presented in Table 5, which shows that the regression of the ricochet angle data was quite good. These equations are valid only for projectiles and plates of the same material, and for angles of obliquity, θ , between 45 and 65 degrees.

RICOCHET PARTICLE SIZE AND VELOCITY ANALYSIS

The next step in the analysis of the oblique impact test specimens was to use crater and hole damage on the ricochet witness plates to determine the sizes and velocities of ricochet debris particles. The following observations were made during inspection of ricochet witness plate damage.

1) Crater dimensions, such as diameter and depth, were found to increase with increasing trajectory obliquity. Penetration depths were observed to decrease with increasing projectile diameter and to increase with increasing original impact velocity.

2) Craters and holes found on ricochet witness plate were approximately circular in shape with very little elongation. This was not very surprising since it had been previously observed that 99% of the impacts occurred at angles of less than 30 degrees with respect to the plane of the bumper plate.

3) Hole diameters were found to increase with increasing trajectory obliquity, and with increasing projectile diameter.

4) The ricochet plates exhibited an excessive amount of dimpling, spalling, and perforation, especially at larger angles of obliquity and higher impact velocities. This damage was concentrated within an angle of 15 degrees with respect to the plane of the bumper plate.

Based on observation (2), it was assumed that normal impact equations for crater depths in thick plates and hole diameters in thin plates could be used in subsequent analyses. However, based on observation (4), it was concluded that equations for penetration depths in thick plates could not be used routinely in the analyses. These equations are, by definition, valid only when there is no spalling or dimpling on the reverse side.

Examination of existing hole diameter equations (ie. those in the Appendix) revealed a strong coupling between particle size and velocity effects. That is, the same size crater can be produced by a small particle travelling at a high speed or by a larger particle travelling at a slower speed. This ambiguity makes exact calculation of ricochet particle sizes and speeds extremely difficult.

However, it was possible to estimate the range of probable ricochet velocites based on an assumed range of probable particle diameters. These velocities were calculated by using the normal impact equations for hole diameters to solve for velocity in terms of all the other quantities. The lower limit of the particle diameter range was set by the limit of applicability of the equations. In most cases, this value was equal to 1.25 mm. For the purposes of this investigation, the upper

limit on the particle size was assumed to be equal to 1/2 of the original projectile diameter. Substitution of appropriate parameters and analysis of the results led to the conclusion that ricochet velocities can exceed 10 km/sec for the smaller particles, but can be as low as 0.5 km/sec for the larger particles. Thus, there is a good probability that some of the the larger ricochet debris particles travel at low velocities. These large low-speed particles can be expected to inflict more serious damage than the smaller ones travelling at higher velocities. In order to understand this phenomenon more fully, further tests will have to be made in which little or no perforation of the ricochet witness plate is allowed to occur. Under these conditions, ballistic limit equations, as well as penetration depth equations, can be used to obtain better estimates of ricochet particle sizes and velocities.

CONCLUSIONS AND RECOMENDATIONS

Several conclusions can be drawn from the analysis of key components in the problem of oblique hypervelocity impact on multi-sheet specimens. These conclusions can have a wide range of consequences on the design of spacecraft meteoroid and space debris protection systems.

First, there exists a critical angle of obliquity. Projectiles with angles of obliquity less than this critical angle produce significant damage to the interior pressure wall and little damage to the ricochet witness plate. Projectiles with trajectory obliquities greater than the critical angle produce little damage to the pressure wall plate, but produce ricochet debris that causes major damage to the ricochet witness plate. This critical angle is estimated to have a value between 60 and 65 degrees. The existance of such an angle has serious consequences on the design and placement of external subsystems such as instrumentation units on spacecraft that are developed for long-duration missions in the meteoroid and space debris environment.

Second, the damage potential of ricochet debris is difficult to extrapolate from existing damage data due to coupling effects of ricochet particle size and velocity. Initial investigations reveal that the velocities of small ricochet debris particles can exceed the original projectile impact velocity while the velocities of larger particles can enter the dangerous low velocity regime. Damage produced by the larger, slower particles was found to be more serious than that produced by the smaller, faster projectiles.

Third, the most serious ricochet damage was found to occur at angles less than 15 degrees with respect to the plane of the bumper plate. For original trajectory obliquities of greater than 60 degrees, the ricochet plate was completely perforated at the bumper plate/ricochet witness plate interface. In general, ricochet damage was found to increase with increases in original trajectory obliquity, original impact velocity, and the size of the original incident projectile.

Fourth, additional experimental and analytical studies are needed in order to be able to more accurately assess the extent of ricochet damage that can be expected to occur as the result of an oblique hypervelocity impact. Several specifics of these future studies are outlined below.

The following recommendations are made for future investigations of oblique hypervelocity impact phenomena.

1) It would be instructive to know at which angles the ricochet particles causing the largest holes or deepest craters strike the witness plate. A preliminary investigation of these angles was performed, but the results were inconclusive. Knowledge of these angles would enable a designer to estimate critical exterior locations and avoid them in the

placement of exterior subsystem components.

2) Future experimental testing of oblique impact should be conducted with ricochet witness plates sufficiently thick so that little or no perforation occurs. In this manner, virtually all the crater damage produced by ricochet particles can be used with thick plate equations to estimate ricochet velocities and particle sizes.

3) A more precise value of the critical angle of obliquity should be made. In order to accomplish this, a more sophisticated damage criterion is needed. It should also be determined whether or not this critical angle is dependent on any material, geometric , or impact parameters.

4) Future experimental investigations should be conducted with projectiles and specimen plates made from different materials. In this manner, the testing will better simulate on-orbit impacts of meteoroids or pieces of space debris with spacecraft materials. Use of a wide variety of materials, including composites, will also serve to improve and expand the applicability of the empirical expressions of the current model.

5) More testing should be done at higher angles of obliquity to complement the large number of tests that have been performed at smaller angles (ie. less than 45 degrees). In light of the existance of a critical obliquity angle near 60 degrees, these tests are essential to be able to fully understand the oblique impact process.

6) Further analyses of spray angles and damage areas due to projectile, bumper plate and ricochet debris particle sprays need to be performed. The inclusion of a thickness term in equations (3) and (4) should be investigated as should the inclusion of an obliquity correction term in equation (1). Information on the scatter of the predictions of the regression equations should also be provided.

7) Extensive analytical investigations of the phenomena involved in oblique hypervelocity impact are strongly recommended. Such investigations would achieve several important goals. First, they would provide verification of the empirical model developed in this study. Second, they would provide reliable means of predicting ricochet damage through accurate estimates of ricochet particle sizes and velocities. Third, they would yield damage criteria that would be applicable in a variety of impact situations.

In conclusion, a preliminary investigation of oblique hypervelocity impact has been successfully performed. A set of empirical equations that can be used to estimate the extent of structural damage due to such an impact has been derived. There is, however, a need for further combined experimental testing and analytical study of the mechanisms involved in oblique hypervelocity impact phenomena. Such investigations would result in more reliable design methodologies for meteoroid and space debris protection systems for future long-duration spacecraft, such as the space station.

REFERENCES

Burch, G.T., 1967, "Multi-plate Damage Study", AF-ATL-TR-67-116, Air Force Armament Library, Elgin Air Force Base, Florida.

Cour-Palais, B.G., 1979, "Space Vehicle Meteoroid Shielding Design", Proceedings of the Comet Halley Micrometeoroid Hazard Workshop., N. Longdon, ed., ESA SP-153, Paris, France, p. 85.

Johnson, W.E., 1969, "Oblique Impact Calculations Using a 3-D Eulerian Code", Proceedings of the AIAA Hypervelocity Impact Symposium, AIAA Pap. No. 69-353.

Kessler, D.J., 1981, "Sources of Orbital Debris and the Projected Environment for Future Spacecraft", J. Spacecraft, v. 18, n. 4, p. 357.

Kessler, D.J., and Su, S.Y., 1985, Orbital Debris, NASA CP 2360, Washington, D.C.

Lundeberg, J.F., Lee, D.H., and Burch, G.T., 1966, "Impact Penetration of Manned Spacecraft", J. Spacecraft, v. 3, n. 2, p. 182.

McMillan, A.R., 1968, "Experimental Investigations of Simulated Meteoroid Damage to Various Spacecraft Structures", NASA CR 915, Washington, D.C.

Maiden, C.J., and McMillan, A.R., 1964, "An Investigation of the Protection Afforded a Spacecraft by a Thin Shield", AIAA Journal, v. 2, n. 11, p. 1992.

Reynolds, R.C., Fisher, N.H., and Rice, E.E., 1983, "Man-Made Debris in Low Earth Orbit - A Threat to Future Space Operations", J. Spacecraft, v. 20, n. 3, p. 179.

Summers, J.L., 1959, "Investigation of High Speed Impact: Regions of Impact and Impact at Oblique Angles", NASA TN D-94, Washington, D.C.

Swift, H.F., Bamford, R., and Chen, R., 1983, "Designing Space Vehicle Shields for Meteoroid Protection: A New Analysis", Adv. Space Res., v. 2, n. 12, p. 219.

Wallace, R.R., Vinson, J.R., and Kornhauser, M., 1962, "Effects of Hypervelocity Particles on Shielded Structures", ARS Journal, p. 1231.

Whipple, E.L., 1947, "Meteoroites and Space Travel", Astron. Journal, v. 52, p. 5.

Wilkinson, J.P.D., 1968, "A Penetration Criterion for Double-Walled Structures Subject to Meteoroid Impact", AIAA Jounral, v. 7, n. 10, p. 1937.

APPENDIX

Thin Plate Hole Diameter Equations for Normal Hypervelocity Projectile Impact

Maiden, Gehring, and McMillan (1963):

$$D/d = 0.45\ V\ (t_S/d)^{0.666} + 0.90 \qquad \text{(A-1)}$$

$$D/d = 2.40\ (V/C)\ (t_S/d)^{0.666} + 0.90 \qquad \text{(A-2)}$$

Sawle (1970):

$$D/d = 3.2\ [(\rho_P/\rho_T)(V/C)]^{0.222}\ (t_S/d)^{0.666} + 1.0 \qquad \text{(A-3)}$$

Nysmtih (1968):

$$D/d = 1.32\ (t_S/d)^{0.45}\ V^{0.50} \qquad \text{(A-4)}$$

Lundeberg, Stern, and Bristow (1965):

$$D/d = 3.4\ (t_S/d)^{0.333}\ (V/C)^{0.333}\ (1.0\text{-}0.0308\rho_T/\rho_P) \qquad \text{(A-5)}$$

Rolsten, Wellnitz, and Hunt (1964):

$$D/d = [2.0 + (\rho_T/\rho_P)^{0.50}]^{0.50} \qquad \text{(A-6)}$$

Notation

D ... hole diamter

d ... projectile diameter

V ... impact velocity

C ... longitudinal wave speed in bumper plate material

t_S ... bumper palte thickness

ρ_P ... projectile material density

ρ_T ... bumper plate material density

Additional References

Lundeberg, J.F., Stern, P.H., and Bristow, R.J., 1965, "Meteoroid Protection for Spacecraft Structures", NASA CR 54201, Washington, D.C.

Maiden, C.J., Gehring, J.W., and McMillan, A.R., 1963, "Investigation of Fundamental Mechanism of Damage to Thin Targets by Hypervelocity Projectiles", GM-DRL-TR-63-225, General Motors Defence Research Laboratory, Santa Barbara, California.

Nysmith, C.R., 1968, "Pentration Resistance of Double Sheet Structures at Velocities to 8.8 km/sec", NASA TN D-4568, Washington, D.C.

Rolsten, R.F., Wellnitz, J.N., and Hunt, H.H., 1964, "An Example of Hole Diameter in Thin Plates Due to Hypervelocity Impact", J. Appl. Physics, v. 33, n. 3, p. 556.

Sawle, D.R., "Hypervelocity Impact on Thin Sheets and Semi-Infinite Targets at 15 km/sec", AIAA Journal, v. 8, n. 7, p. 1240.

Acknowledgements

The author wishes to acknowledge the support of the NASA/ASEE Summer Faculty Fellowship Program along with Gerald Karr, the UAH Director, and Ernestine Cothran, the MSFC Program Co-Director.

The author's gratitude is extended to Roy Taylor, Chief of the Laboratory Support Branch of the Engineering Physics Division of the Materials and Processes Laboratory for his support and guidance.

Test No.	V (km/sec)	D (mm)	θ (deg)	D_{min} (mm)	D_{max} (mm)	Eccen-tricity	θ_1 (deg)	θ_2 (deg)	α_c (deg)	α_{99} (deg)
EH1A	7.07	7.95	30	16.0	17.0	1.06	****	24.8	****	****
EH1B	6.96	7.95	45	16.5	20.0	1.22	10.9	38.1	15.5	29.2
EH1C	7.14	7.95	60	16.5	24.9	1.51	9.6	50.0	11.2	27.6
EH1D	7.18	7.95	75	14.5	36.1	2.49	4.7	26.9	7.9	27.1
EHCP	7.58	4.75	75	10.0	18.0	1.82	4.7	20.9	8.2	25.6
135C	6.76	6.35	30	13.2	14.2	1.08	****	24.0	****	****
135D	6.93	6.35	30	13.2	14.2	1.08	****	27.0	****	****
136A	6.25	6.35	55	14.0	18.3	1.31	10.7	43.5	8.7	23.3
136B	7.30	6.35	55	14.0	20.1	1.44	10.1	41.8	11.9	28.3
136C	6.67	6.35	55	13.5	17.0	1.26	11.0	38.2	12.9	28.4
150A	7.08	6.35	45	14.2	18.0	1.26	10.0	39.0	11.0	24.0
157A	7.40	4.75	60	13.7	17.3	1.26	9.3	36.0	8.0	22.0
162A	6.49	4.75	30	11.9	14.0	1.18	****	21.0	****	****
162B	5.03	4.75	30	9.9	11.7	1.17	****	27.0	****	****
206F	6.24	4.75	45	11.7	13.5	1.16	8.0	31.0	8.0	21.0
208E	6.48	6.35	65	13.0	21.0	1.61	9.0	47.0	8.0	20.0
209D	7.40	6.35	65	14.5	19.6	1.36	****	****	11.0	27.0
230C	5.16	6.35	45	12.4	16.0	1.28	10.0	34.0	11.0	26.0
230D	5.59	6.35	45	13.5	16.3	1.22	10.0	37.0	10.0	25.0
230E	6.62	6.35	45	14.2	17.5	1.25	10.0	32.0	12.0	25.0
231C	6.59	7.95	65	16.5	31.0	1.87	8.7	55.7	8.4	20.4
231D	7.26	7.95	65	16.5	25.9	1.57	10.2	49.7	9.7	23.0

Table 1 -- Impact Test Data

	Maiden et.al.		Sawle	Nysmith	Lundeberg et.al.	Rolsten et.al.
	(A-1)	(A-2)	(A-3)	(A-4)	(A-5)	(A-6)
Average Error (%)	-4	-1	+14	-16	+7	-15
Standard Deviation (%)	6	6	17	5	9	14

Table 2 -- Minimum Hole Dimension Predictions, Normal Impact Equations

****

	$\%\varepsilon_{avg}$	$100R^2$
D_{min}/D	-0.001	78.7
D_{max}/D	0.000	75.2

Table 3 -- Regression Analysis of Bumper Hole Dimension Data Error Summary

		% ϵ_{avg}	$100R^2$
As functions of hole parameters	θ_1/θ	0.236	86.5
	θ_2/θ	0.269	50.2
As functions of imp. parameters	θ_1/θ	0.312	82.1
	θ_2/θ	0.226	57.7

Table 4 -- Regression Analysis of Penetration Angle Data Error Summary

****

		% ϵ_{avg}	$100R^2$
As functions of hole parameters	α_c/θ	0.968	77.5
	α_{99}/θ	0.463	81.1
As functions of imp. parameters	α_c/θ	0.779	81.9
	α_{99}/θ	0.548	77.6

Table 5 -- Regression Analysis of Ricochet Angle Data Error Summary

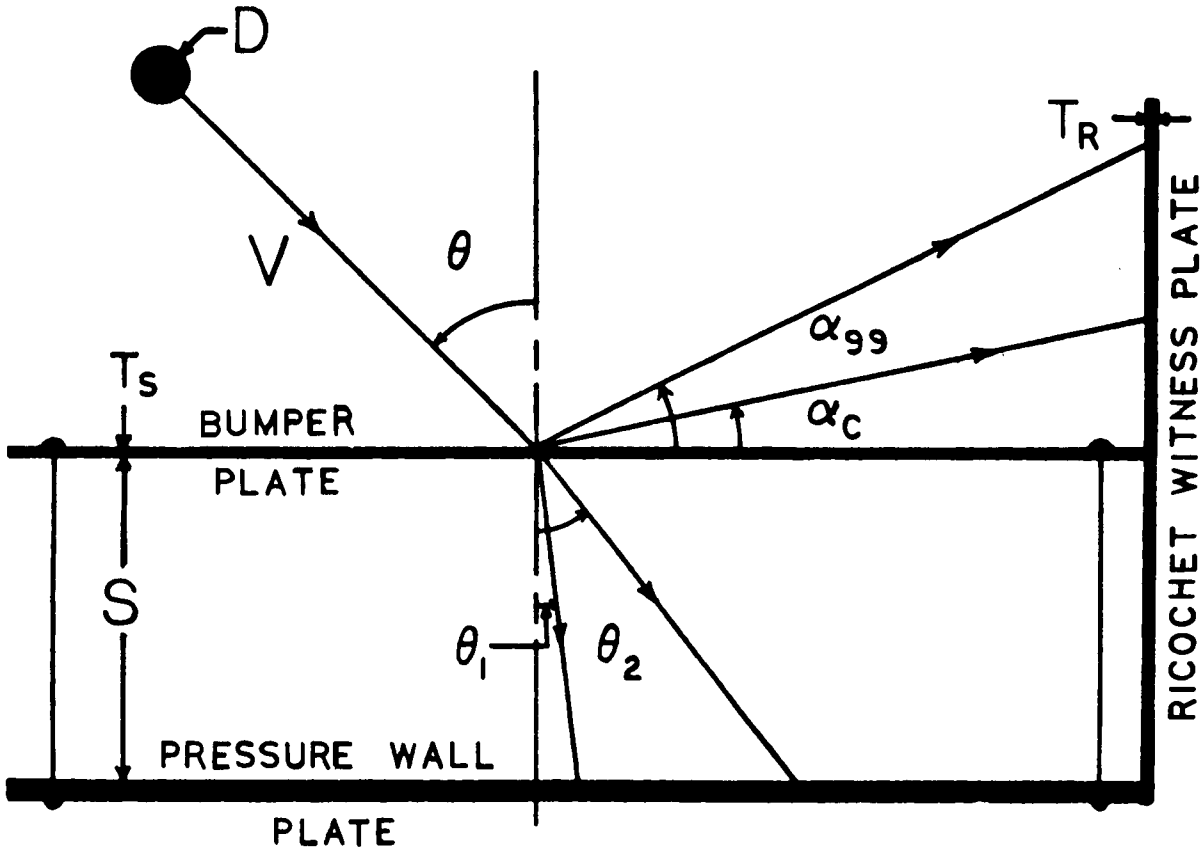

Figure 1 -- Test Configuration and Definitions

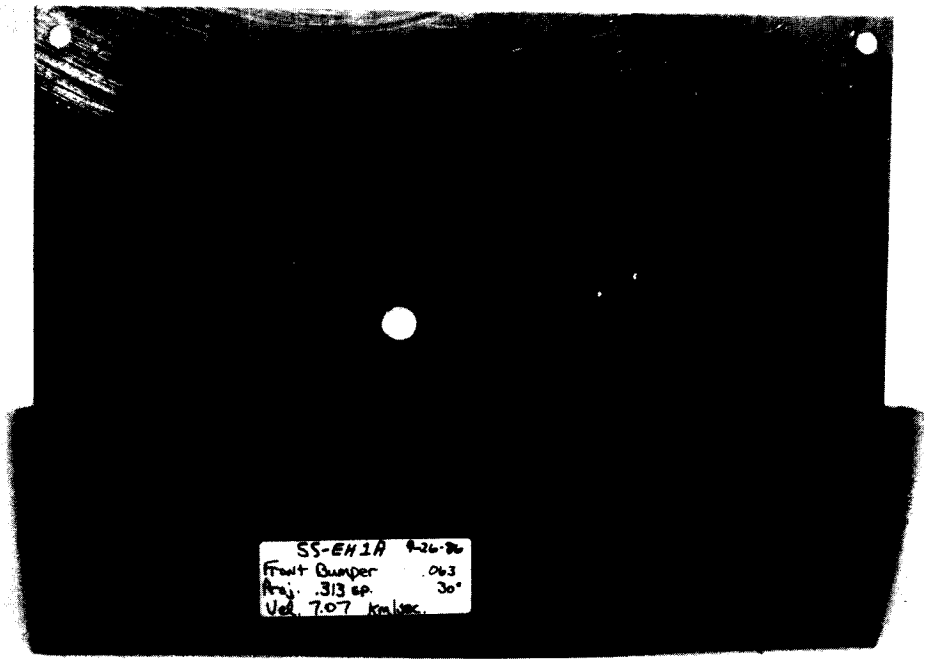

Figure 2a

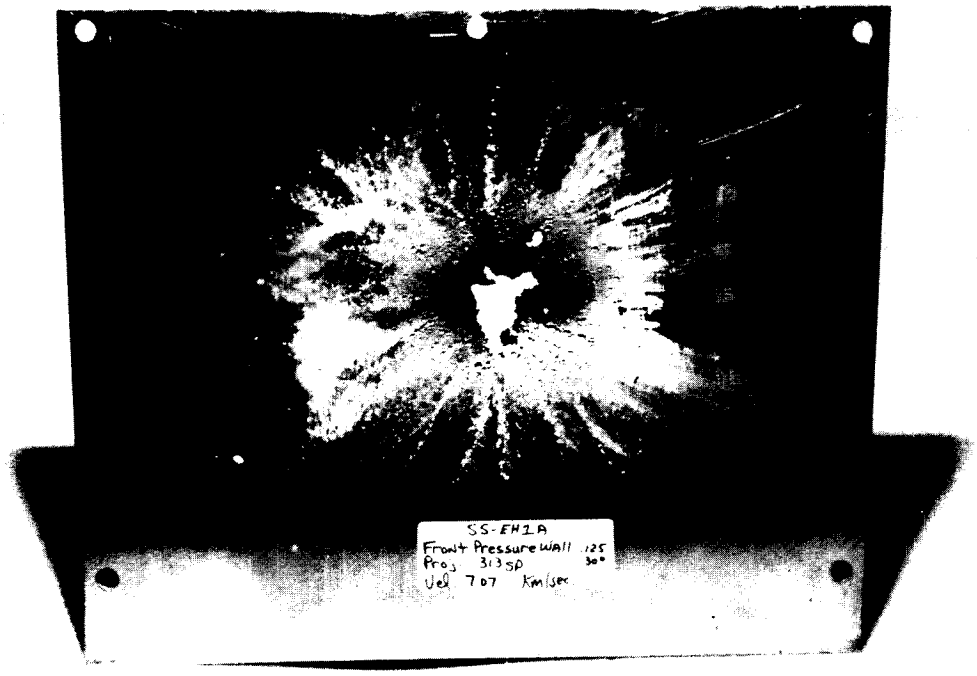

Figure 2b

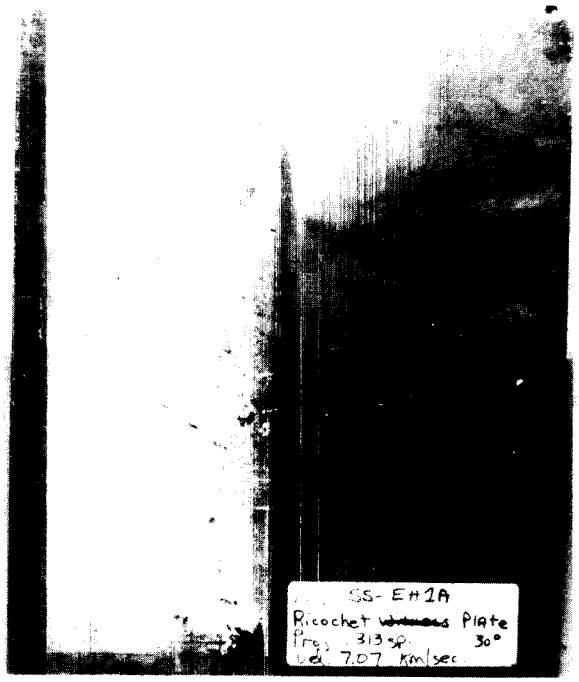

Figure 2c

Figure Captions

Figure 2a -- 30-deg Impact (EH1A)
Bumper Plate

Figure 2b -- 30-deg Impact (EH1A)
Pressure Wall Plate

Figure 2c -- 30-deg Impact (EH1A)
Ricochet Witness Plate

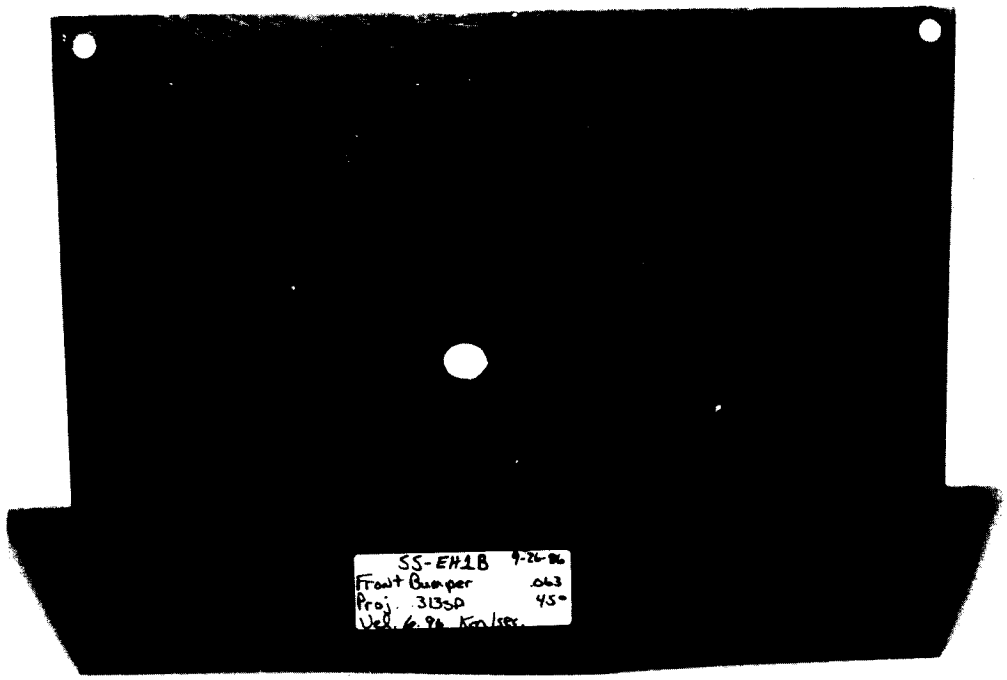

Figure 3a

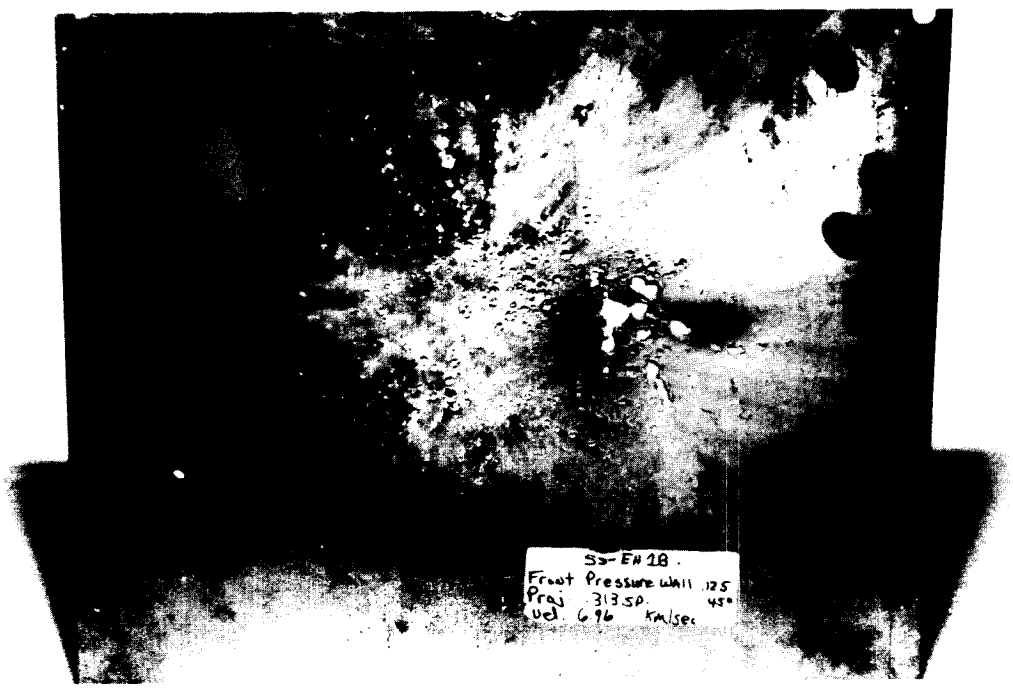

Figure 3b

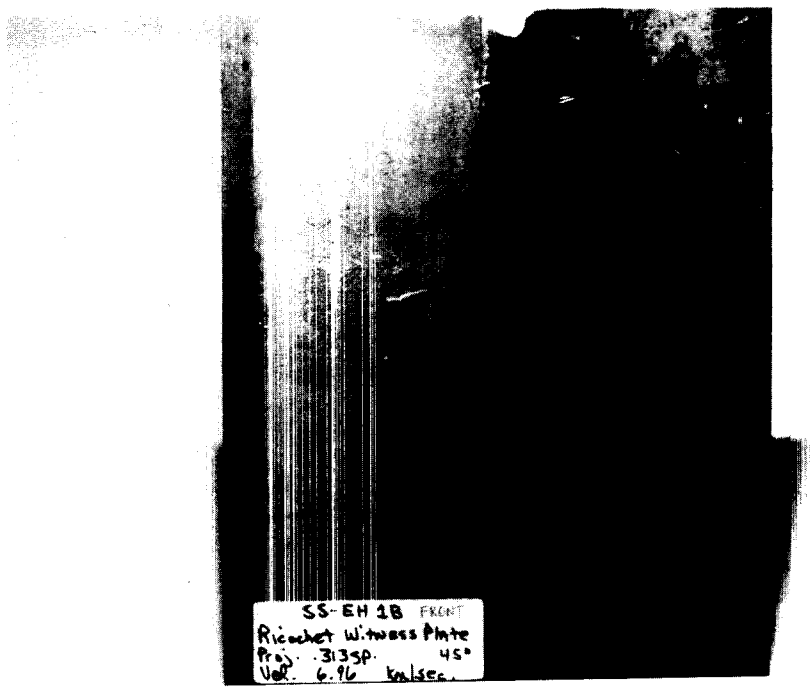

Figure 3c

Figure Captions

Figure 3a -- 45-deg Impact (EH1B)
Bumper Plate

Figure 3b -- 45-deg Impact (EH1B)
Pressure Wall Plate

Figure 3c -- 45-deg Impact (EH1B)
Ricochet Witness Plate

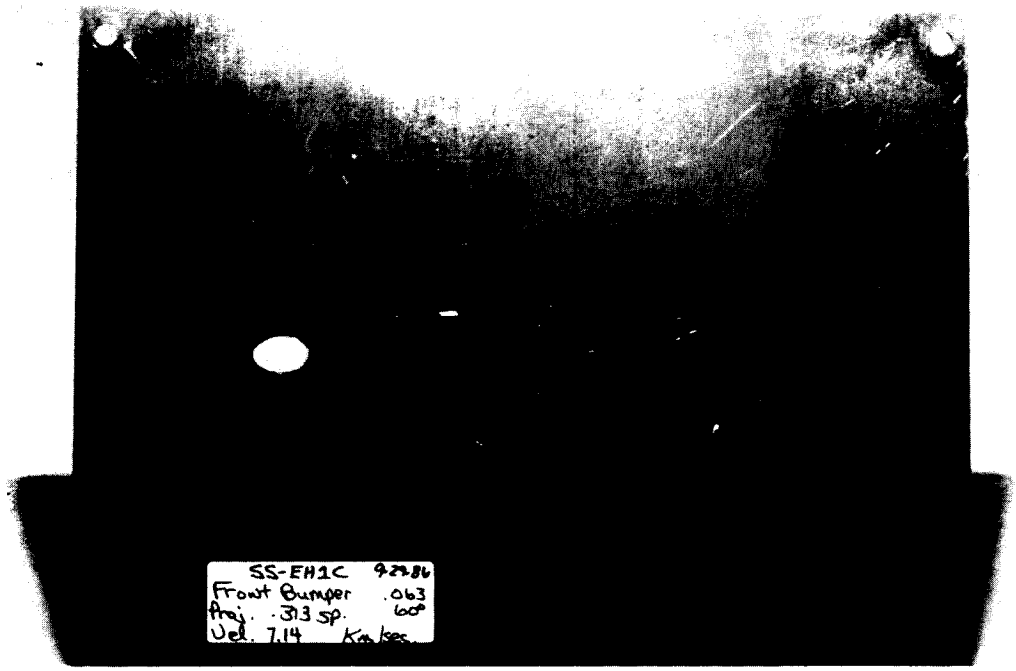

Figure 4a

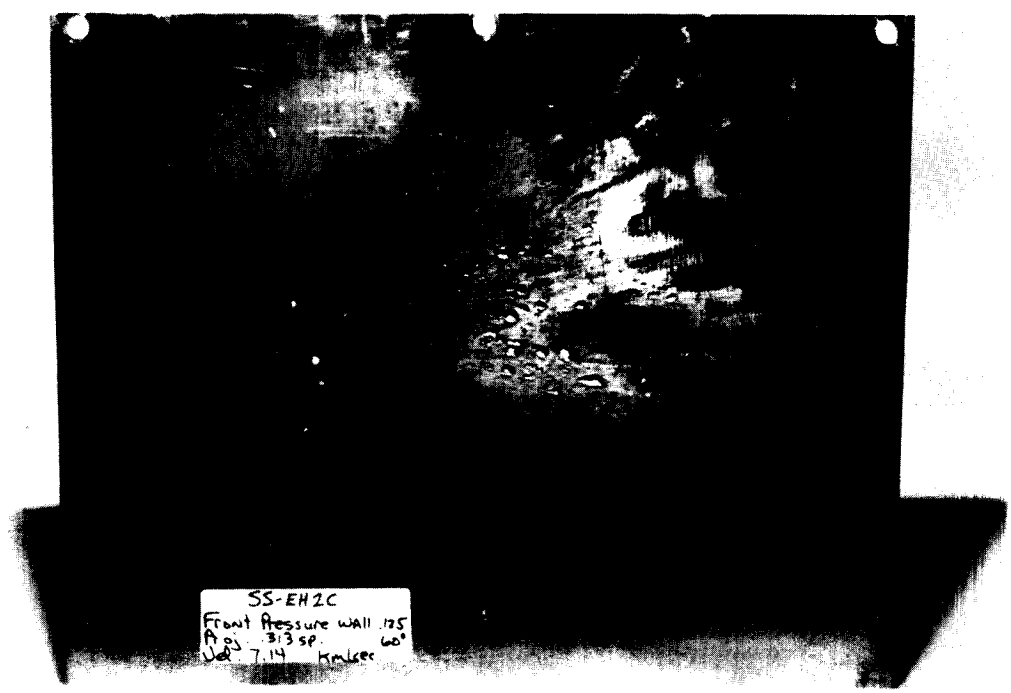

Figure 4b

Figure 4c

Figure Captions

Figure 4a -- 60-deg Impact (EH1C)
Bumper Plate

Figure 4b -- 60-deg Impact (EH1C)
Pressure Wall Plate

Figure 4c -- 60-deg Impact (EH1C)
Ricochet Witness Plate

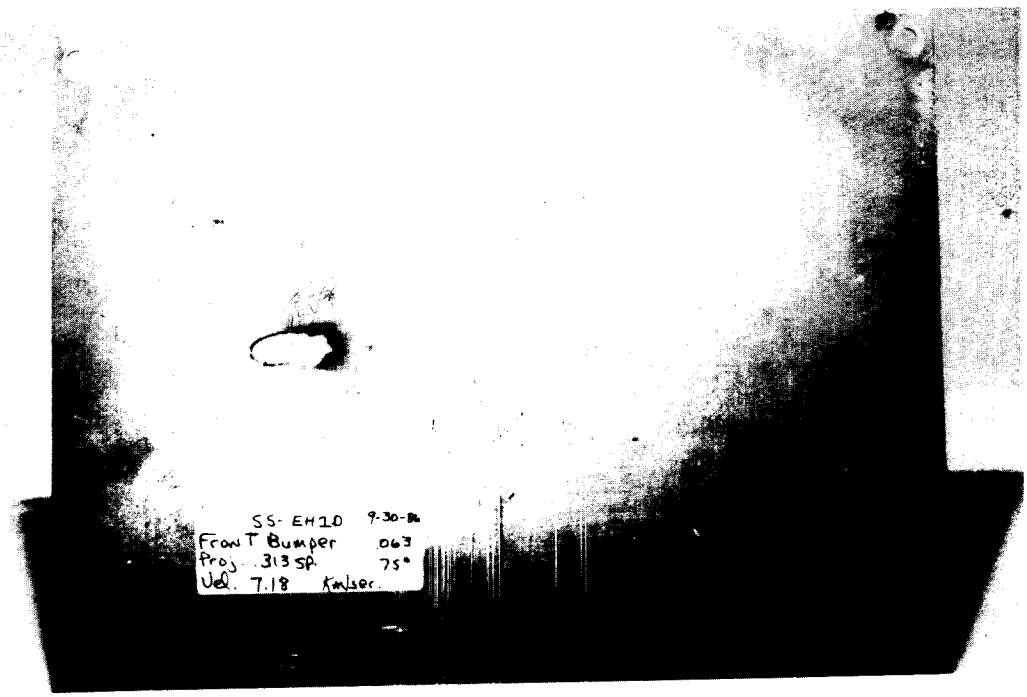

Figure 5a

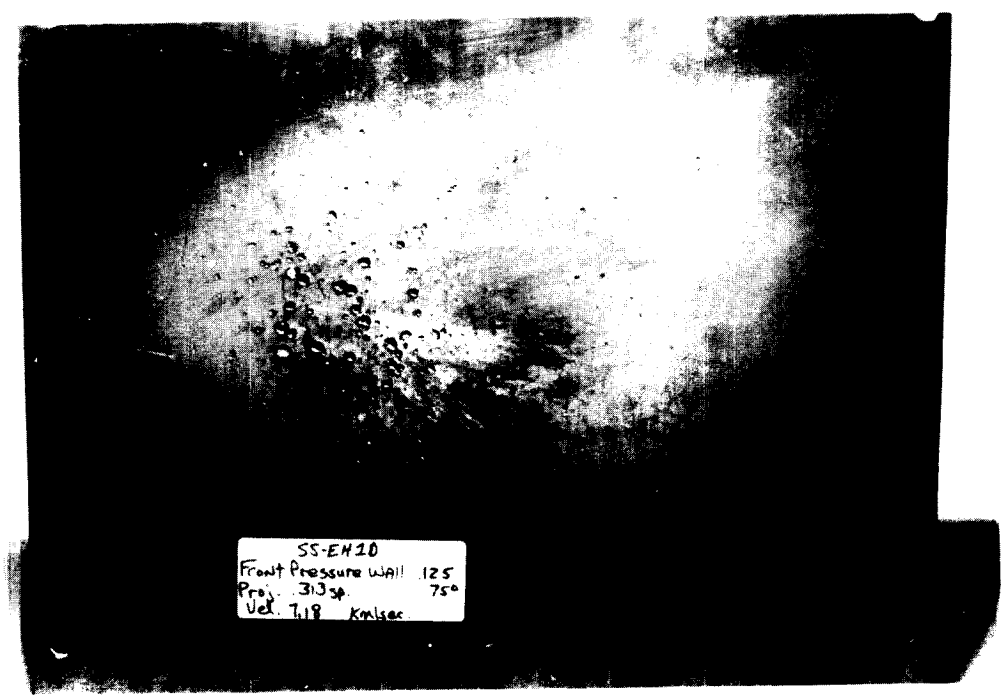

Figure 5b

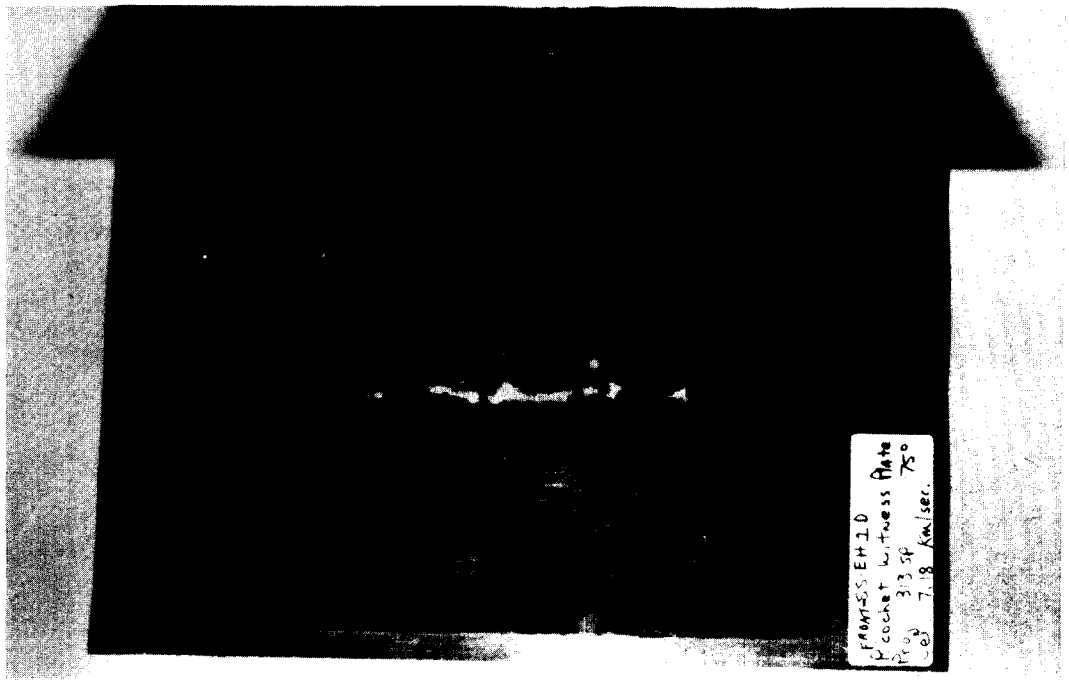

Figure 5c

Figure Captions

Figure 5a -- 75-deg Impact (EH1D)
Bumper Plate

Figure 5b -- 75-deg Impact (EH1D)
Pressure Wall Plate

Figure 5c -- 75-deg Impact (EH1D)
Ricochet Witness Plate

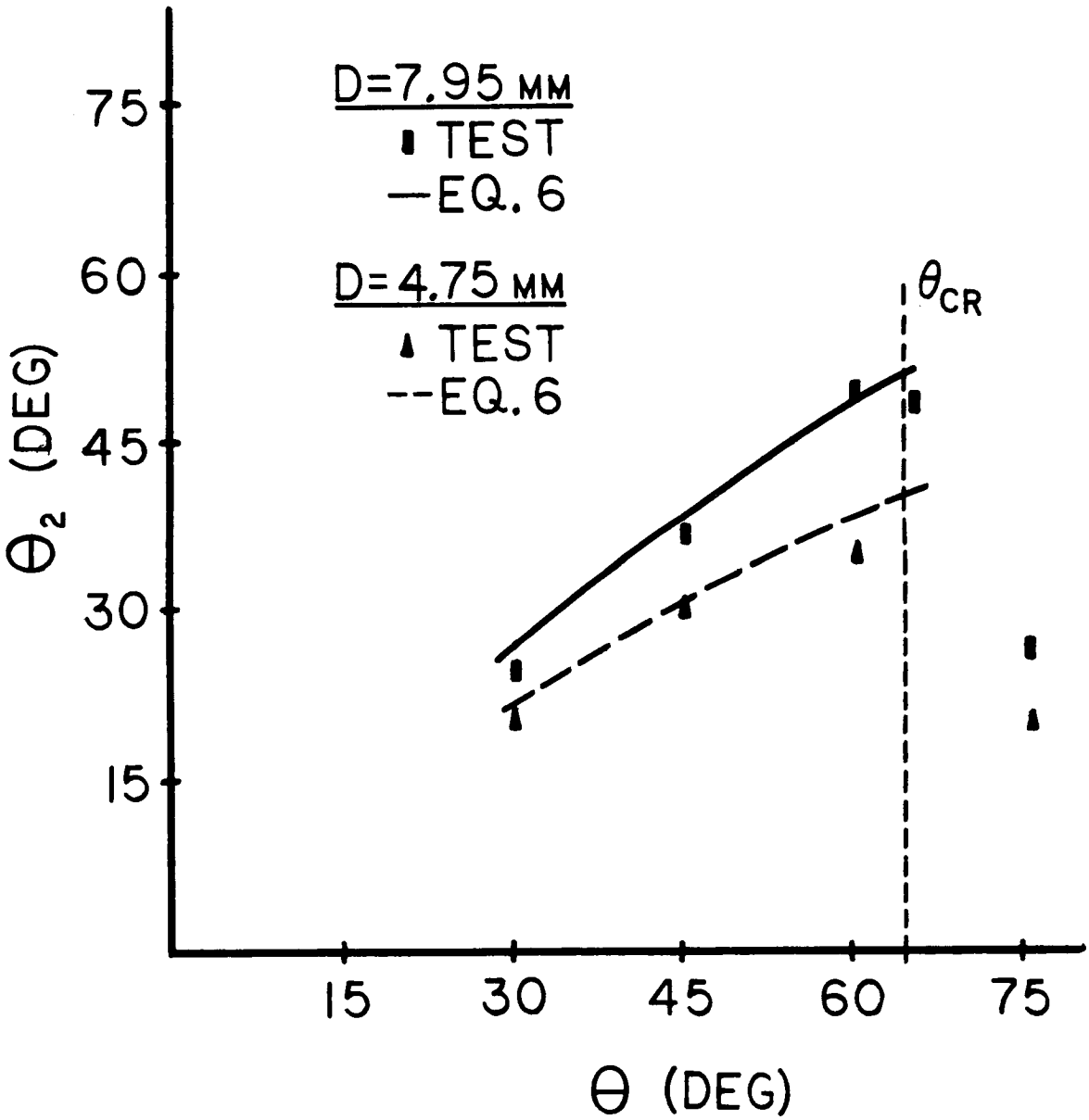

Figure 6 -- 'In-Line' Projectile Particle Trajectory:
Test Data Compared With
Regression Equation Predictions
(V=7 km/sec)